Free Radical Research, January 2008; 42(1): 49–56

informa
healthcare

Spin labelling of *Bacillus anthracis* endospores: A model for *in vivo* tracking by EPR imaging

PEI TSAI[1,2,3], GUAN-LIANG CAO[1,2,3], TOD J. MERKEL[4], & GERALD M. ROSEN[1,2,3]

[1]*Department of Pharmaceutical Sciences, University of Maryland School of Pharmacy, Baltimore, MD 21201, USA,* [2]*Medical Biotechnology Center, University of Maryland Biotechnology Institute, Baltimore, MD 21201, USA,* [3]*Center for EPR Imaging In Vivo Physiology, University of Maryland School of Pharmacy, Baltimore, MD 21201, USA, and* [4]*Laboratory of Respiratory and Special Pathogens, Center for Biologics Evaluation and Research, FDA, 8800 Rockville Pike Bethesda, MD 20892, USA*

Accepted by Prof. Michael Davis

(Received 29 August 2007; revised 29 October 2007)

Abstract
Anthrax is caused by the gram-negative bacterium, *Bacillus anthracis*. Infection by this microbe results from delivery of the endospore form of the bacillus through direct contact, either topical or inhalation. With regard to the latter route of administration, it is proposed that endospores of *B. anthracis* enter the lungs and are phagocytized by host alveolar macrophages. Thereafter, it is unclear as to how endospores travel to distal loci and what tissues are the targets. Herein, this study describes the spin labelling of endospores through two different approaches with various aminoxyls. Indeed, after exposure to RAW 264.7 cells, these aminoxyl-containing endospores were phagocytized, as demonstrated by EPR spectroscopy of the infected macrophage, thus providing a potential tool for EPR imaging in animals.

Keywords: Bacillus anthracis, *electron paramagnetic resonance spectroscopy, maleimide-containing aminoxyls, acetoxymethoxycarbonyl-containing aminoxyls*

Introduction

Bacillus anthracis is a spore-forming, Gram-positive organism that is the aetiologic agent of anthrax [1]. According to the current model of *B. anthacis* pathogenesis, endospores enter the lungs, are phagocytized by host alveolar macrophages and are subsequently carried to regional lymph nodes [2–7]. Endospores germinate inside the host macrophage and become vegetative bacilli, which replicate within the phagocyte and some eventually are released from these phagocytes [4–6,8,9]. Bacilli multiply in the lymphatic system and enter the bloodstream where these microbes proliferate to high levels, e.g. 10^7–10^8 organisms/mL blood [10]. This model, however, is speculative. Little is known about the progression of disease following inhalation of endospores. The mechanism and route of transit of endospores of *B. anthracis* from the lungs to distal sites is not clear and the identity of the host cells involved is unknown, although both alveolar macrophages and resident lung dendritic cells have been implicated. Thus, characterization of the mechanism by which endospores in the lung traffic to distal sites and initiate systemic infection would greatly enhance our understanding of the early stages of this disease.

Visualizing *B. anthracis* endospores in whole animals in real-time without sacrificing the animal would greatly enhance our ability to study the progression of

Correspondence: Gerald M. Rosen, PhD, Department of Pharmaceutical Sciences, University of Maryland School of Pharmacy, 725 West Lombard Street, Baltimore, MD 21201, USA. Tel: +1 410 706 0514. Fax: +1 410 706 8184. Email: grosen@umaryland.edu

ISSN 1071-5762 print/ISSN 1029-2470 online
DOI: 10.1080/10715760701787701

anthrax. Animals could be observed to identify the organs and tissues in which endospores are to be found. Through the observation of multiple infections in individual animals, it should be possible to establish the typical trafficking of endospores following aerosol infection. Once data are obtained, assessment of the impact of pre-exposure vaccine therapy on the course of disease can be made in a more rigorous manner than simply assessing mortality.

With the development of low-frequency electron paramagnetic resonance (EPR) spectroscopy [11] and the ability to detect paramagnetic species *in situ*, *in vivo* and in real time [12], tracking *B. anthracis* endospores by EPR imaging in living animals is now a real possibility. First, however, we need to design methods that incorporate a paramagnetic compound, e.g. an aminoxyl, into endospores. In this report, we describe two different strategies, approach A and approach B, in which we are able to spin label endospores with dissimilar groups of aminoxyls (1, 2, 3 and 4 for approach A; and 5 for approach B) at concentrations sufficient, in the case of approach B, that we believe can localize endospores *in vivo*, following aerosol infection of macrophages.

Materials and methods

Materials

All chemical reagents and solvents were obtained from commercial vendors and used without further purifications. IR spectra were recorded on a FT-IR spectrometer (Perkin-Elmer, Norwalk, CT) in $CHCl_3$. Melting points were obtained on a Thomas Hoover capillary melting point apparatus and were corrected.

4-Maleimido-2,2,6,6-tetramethyl-1-piperidinyloxyl (1), 3-maleimido-2,2,5,5-tetramethyl-1-pyrrolidinyloxyl (2), 3-[2(2-maleimidoethoxy)ethylcarbamoyl]-2,2,5,5-tetramethyl-1-pyrrolidinyloxyl (3) and (2-maleimidoethylcarbamoyl)-2,2,5,5-tetramethyl-1-pyrrolidinyloxyl (4) were purchased from Aldrich Chemical Company (Milwaukee, WI).

Synthesis

Preparation of *cis*-3,4-dicarboxy-2,2,5,5-tetramethyl-1-pyrrolidinyloxy (5) and *cis*-3,4-di(acetoxymethoxycarbonyl)-2,2,5,5-tetramethyl-1-pyrrolidinyloxyl (6) are detailed below. Structures of aminoxyls (1-6) are presented in Figures 1 and 2.

3,4-Dicyano-2,2,5,5-tetramethyl-1-pyrrolidinyloxyl (8). To a solution of 3-cyano-2,2,5,5-tetramethyl-1-pyrrolinyloxyl (7) (3.2 g, 14.4 mmol, prepared as described by Rozantzev [14]) in 95% ethanol (100 mL) was added to 100 mL of an aqueous solution of potassium cyanide (3.05 g, 46.9 mmol) and ammonium chloride (2.6 g, 49.1 mmol). This mixture was heated at 70°C for 7 h, at which point the reaction mixture was cooled to room temperature. The solution was then saturated with NaCl and extracted with ether (5×100 mL). The combined ether solutions were dried over anhydrous $MgSO_4$, filtered and reduced to dryness using a rotary evaporator. The resulting mixture was purified using silica gel 60 (200–340 mesh). A small amount of starting material, aminoxyl (7), was removed by elution with hexane-ether (2:1). Subsequent elution with hexane-ether (1:1) yielded *trans*-3,4-dicyano-2,2,5,5-tetramethyl-1-pyrrolidinyloxyl (8a) (1.7 g, 46%), mp 141–142°C

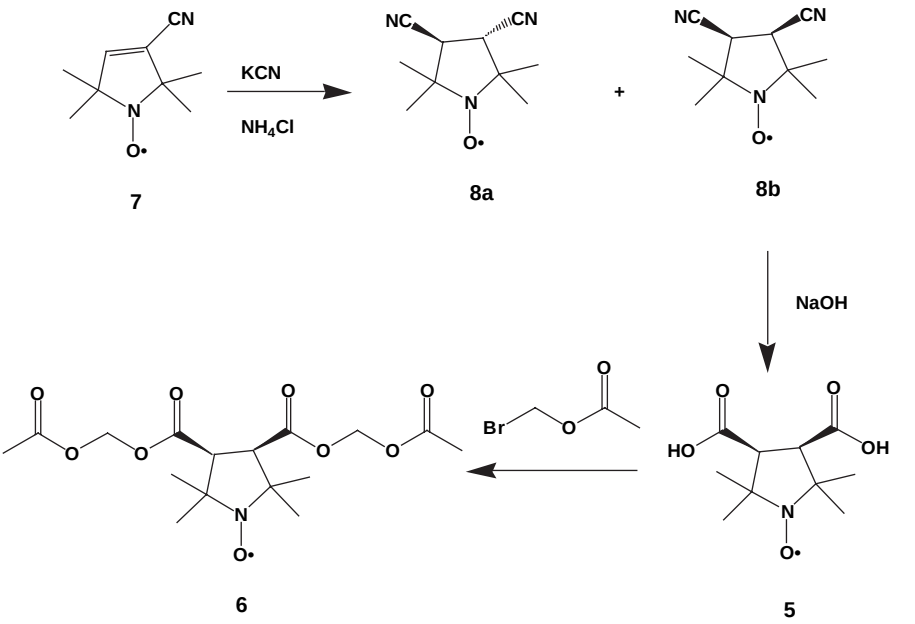

Figure 1. Synthetic scheme for aminoxyls 5 and 6.

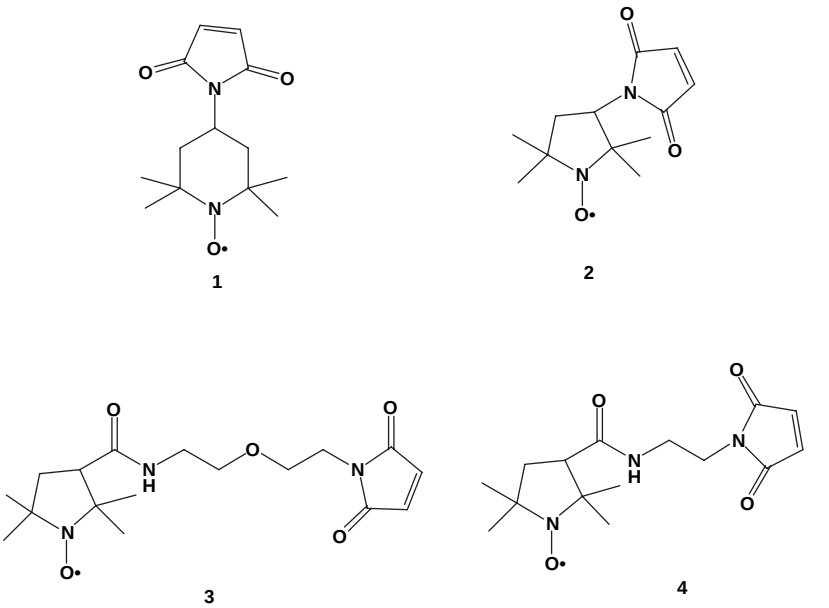

Figure 2. Structures of the maleimide-containing aminoxyls used for covalently labelling of endospores (Apporach A).

(from ether-hexane); IR ($CHCl_3$): ν_{max}/cm 2215 (CN). Increasing the polarity of the solvent to hexane-ether (1:2) afforded *cis*-3,4-dicyano-2,2,5,5-tetramethyl-1-pyrrolidinyloxyl (8b) (0.7 g, 18%), mp 84°C (from ether-hexane) IR ($CHCl_3$): ν_{max}/cm 2220 (CN)(preparative scheme shown in Figure 1) [15].

Cis-3,4-di(acetoxymethoxycarbonyl)-2,2,5,5-tetramethyl-1-pyrrolidinyloxyl (6). A mixture of *cis*-3,4-dicyano-2,2,5,5-tetramethyl-1-pyrrolidinyloxyl (8b) (1 g, 5.2 mmol) and 2 M NaOH (60 mL) was warmed to 90°C for 3 days, at which point the reaction was cooled and the aqueous solution extracted with ether. The remaining aqueous solution was cooled in an ice bath, acidified with 10% HCl and extracted with ether. This organic solution was dried over anhydrous $MgSO_4$, filtered and rotary evaporated to dryness, leaving a light yellow solid. Recrystallization from acetone-benzene afforded *cis*-3,4-dicarboxy-2,2,5,5-tetramethyl-1-pyrrolidinyloxyl (5) (0.9 g, 79%, mp = 228–230°C with decomposition) (Figure 1).

To a mixture of *cis*-3,4-dicarboxy-2,2,5,5-tetramethyl-1-pyrrolidinyloxyl (5) (0.4 g, 1.7 mmol) and K_2CO_3 (0.7 g, 5.1 mmol) in DMSO (2 mL) was added bromomethyl acetate (0.56 g, 0.34 mL, 3.4 mmol, Aldrich Chemical Co., Milwaukee, WI). The reaction was stirred at room temperature for 3 h, at which point CH_2Cl_2 (50 mL) was added. This mixture was washed with water (3×100 mL). The organic solution was dried over anhydrous Na_2SO_4, filtered and reduced to dryness on a rotary evaporator. The residual DMSO was removed under high vacuum to give yellow oil, which solidified overnight. The compound was recrystallized from boiling petroleum ether to which diethyl ether was added dropwise to dissolve the solid, affording *cis*-3,4-di(acetoxymethoxycarbonyl)-2,2,5,5-tetramethyl-1-pyrrolidinyloxyl (6) (0.50 g, 80%) (Figure 1), mp 84–85°C; IR ($CHCl_3$): ν_{max}/cm 1769 br (CO). Found: C, 51.29; H, 6.38; N, 3.72. $C_{16}H_{24}NO_7$ requires C, 51.34; H, 6.46; N, 3.74.

EPR spectroscopic measurement

For EPR spectroscopic measurement, each sample was added to a quartz flat cell, which was then introduced into the cavity of the spectrometer (model E-109, Varian Associates, Palo Alto, CA). EPR spectra were collected using EWWIN 32, version 5.23 (Scientific Software Services, 42583 Five Mile Road, Plymouth, MI). EPR spectra were recorded at room temperature with the following instrumental settings: microwave power, 20 mW; field set, 3330 G; sweep width, 100 G; modulation frequency, 100 kHz; modulation amplitude, 0.5 G; response time, 0.5 s; sweep, 12.5 $Gmin^{-1}$. Receiver gain ranged from $2 \sim 10 \times 10^4$.

Preparation of endospore labelled with aminoxyl

Δ*Ger H B. anthracis* endospores were prepared as described previously [13]. A single colony harvested from an overnight culture grown on L-agar at 37°C was used to inoculate 100 mL of L-broth in a 250-ml conical flask. The culture was incubated at 37°C on an orbital shaker (200 rpm) for 6 h. At the end of this period, 3 mL of culture was transferred to a 225 cm^2 vented tissue flask (Corning Inc) containing 175 mL isolation agar. Following inoculation, flasks were incubated at 37°C until 99–100% of the bacilli had formed endospores (microscopic examination/phase

contrast). The% spore yield was determined by comparing colony counts of heated (60°C for 60 min) and unheated samples. Endospores were harvested by adding 20 ml of sterile PBS to the flask. The resuspended endospores from 20 flasks were pooled and centrifuged at 4200 rpm for 10 min at 4°C. The resulting pellet was resuspended in 200 mL of sterile PBS and centrifuged again. This procedure was repeated a total of 10 times with endospores being resuspended in a final volume of 50 mL, which was refrigerated at 4°C. The final endospore stock concentration was determined to be 1×10^9 spores/mL. Endospores used for experimentation were heat shocked at 60°C for 60 min to kill any remaining bacilli.

Endospores (3×10^7/mL) were incubated at 37°C for 3 h with aminoxyls (1, 2, 3, 4) (5 mM, 0.5% DMSO, final concentration) and at 37°C for 18 h with aminoxyls (5, 6) (5 mM, 0.5% DMSO, final concentration) in the shaking bath. The mixture (0.5 mL) was then washed six-times with PBS buffer (5 mL, pH = 7.2) and the supernatant each time was discarded after centrifugation at 4200 rpm. The 6th wash was saved for measuring of any remaining aminoxyl. At this point the endospore pellet was suspended to a final total volume of 0.5 mL for EPR spectroscopic measurement.

RAW264.7 cell culture preparation

Cell culture media and supplements were obtained from Life Technologies, Invitrogen (Carlsbad, CA). The murine macrophage cell line, RAW264.7, was obtained from American Type Culture Collection (Catalogue # TIB-71, Manassas, VA). These cells were cultured in DMEM supplemented with 10% heat-inactivated foetal bovine serum containing penicillin (100 U/mL) and streptomycin (100 μg/mL) at 37°C in a 5% CO_2, 95% air-humidified incubator. At the time of the experiment, cells were cultured in six-well plate with fresh media. The next day, the cells were treated with the aminoxyls.

Loading of RAW264.7 cells with aminoxyl-labelled/entrapped endospores

Into each well containing RAW264.7 cells (5×10^6/mL) was added the aminoxyl-labelled/entrapped endospore (5×10^6/mL) and the mixture was incubated for 18 h at 37°C. The supernatant was removed and then 3 ~ 5 mL of PBS (pH = 7.2) was added and swirled gently for ~ 2 min and the supernatant was discarded. This procedure was repeated six-times. The pellet was then suspended and transferred to a 15 mL centrifuge tube and centrifuged at 1000 rpm. The supernatant was saved to determine that the remaining solution was free of the aminoxyl-containing endospore. The pellet was then suspended in PBS (pH = 7.2) to a total of 0.5 mL for EPR spectroscopic measurement. Similarly, the control experiment with aminoxyls (1, 6) (1 μM) with RAW264.7 cells was conducted following the same procedure. To determine the effect cytochalasin D has on phagocytic uptake of aminoxyl-containing endospores, the procedure above was followed; however, in this case, RAW264.7 cells pre-treated with cyctochalasin D (10 μg/mL) were used.

Results and discussion

Labelling endospores of B. anthracis *with maleimide-containing aminoxyls (Approach A)*

A number of years ago, we described the efficient labelling of *Neisseria gonorrhoeae* with a maleimide-functionalized aminoxyl, as thiol-containing proteins in this microbe reacted with the maleimido group, attaching covalently the aminoxyl to this bacterium [16]. We considered that this approach might be a reasonable avenue by which to label the endospore of *B. anthracis* given that this bacterium has at least 20 different proteins, a number of which are tightly associated with an exosporium, including alanine racemase, inosine hydrolase, GroEL, ExsF, CotY, ExsY, CotB and a novel protein, named ExsK [17]. Undoubtedly, some of these proteins have sulphydryl groups. Thus, we decided to explore the possibility of labelling endospores of *B. anthracis* with maleimide-containing aminoxyls.

In our initial series of experiments, we incubated endospores of *B. anthracis* (3×10^7/mL) with 4-maleimido-2,2,6,6-tetramethyl-1-piperidinyloxyl (1) (Figure 2) (5 mM, 0.5% DMSO, final concentration) for 3 h at 37°C. After extensively washing the mixture, the last washout did not contain aminoxyl (1). The EPR spectrum of endospore-covalently labelled aminoxyl is typical of aminoxyls, which have been covalently attached to proteins in cells where restricted motion broadens the spectral lines (Figure 3A) [16]. The anisotropic hyperfine interactions of the bound aminoxyl showed different classes of bound spin-label, representing differing degrees of immobilization [16]. We suspect that aminoxyl (1) covalently labelled a number of different thiol-containing proteins, which was the source of the anisotropy observed in Figure 3A.

Next we decided to label endopsores with a 5-membered ring aminoxyl-containing maleimide. When 3-maleimido-2,2,5,5-tetramethyl-1-pyrrolidinyloxyl (2) (5 mM, 0.5% DMSO, final concentration) was incubated with endospores of *B. anthracis* (3×10^7/mL), the resultant EPR spectrum of aminoxyl (2), which was also covalently labelled therein (Figure 3B), was substantially smaller than that found for aminoxyl (1). This was a surprising finding; given that there are thiols in the exosporium and that 6-membered ring aminoxyls are 10-times more prone to thiol-mediated reduction than are 5-membered

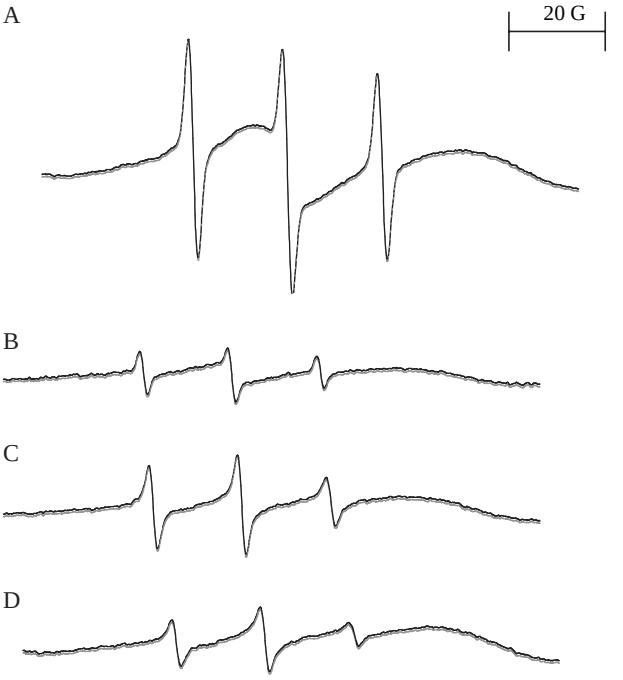

Figure 3. EPR spectra of covalently-labelled endospores with different aminoxyls. (A) Aminoxyl (1); (B) Aminoxyl (2); (C) Aminoxyl (3); (D) Aminoxyl (4). Data shown are the average of 10 scans. Instrumental settings: microwave power, 20 mW; field set, 3330 G; sweep width, 100 G; modulation frequency, 100 kHz; modulation amplitude, 0.5 G; response time, 0.5 s; sweep, 12.5 $Gmin^{-1}$; and receiver gain 10×10^4.

aminoxyls [18], as reviewed in Kocherginsky and Swartz [19]. Hence, we thought that the difference in labelling efficiency was due to steric hindrance, the close proximity of the five-membered aminoxyl ring with methyl groups at position 2 adjacent to the maleimide at position 3 to which thiol-containing proteins in the exosporium would covalently attach thereto. We reasoned that this steric hindrance may be avoided by increasing the chain length between the aminoxyl and the maleimide group and enhanced efficiency of labelling endospores would result. We, therefore, expected that endospores, which were covalently labelled with either 3-[2 (2-maleimidoethoxy)ethylcarbamoyl]-2,2,5,5-tetramethyl-1-pyrrolidinyloxyl (3) or (2-maleimidoethylcarbamoyl)-2,2,5,5-tetramethyl-1-pyrrolidinyloxyl (4), would exhibit an increase in the EPR spectral peak heights. However, as shown in Figure 3C and D, this was not the case. In fact, increasing the chain length between the aminoxyl and the attachment group had no impact on endospore-labelling efficiency, as there was no significant difference in EPR spectral peak heights whether endospores were labelled with aminoxyl (2), aminoxyl (3) or aminoxyl (4). We, then, pursued an alternative approach to increase the concentration of an aminoxyl in the endospore.

Entrapping endospores of B. anthracis *with carboxy-containing aminoxyls (Approach B)*

Several years ago, we reported that 3-acetoxymethoxycarbonyl-2,2,5,5-tetramethyl-1-pyrrolidinyloxyl (9) crossed cell membranes, where upon esterase hydrolysis 3-carboxy-2,2,5,5-tetramethyl-1-pyrrolidinyloxyl (10) was entrapped, accumulating to high intracellular concentrations [20] (Figure 4). As one of the functions of the exosporium is to protect the endospore from an environment that may compromise survival of the microbe, we would expect that aminoxyl-containing acetoxymethoxycarbonyl esters, such as compound (6), might diffuse into the exposorium, where one of the hydrolases, reported to be therein [17], would hydrolyse an acetoxymethoxycarbonyl ester to the corresponding carboxylic acid (Figure 5). In contrast, we envision that endospores treated with the carboxylic acid would not accumulate, as the anion of the aminoxyl would remain extracellular (Figure 5).

Thus, we synthesized *cis*-3,4-di(acetoxymethoxycarbonyl)-2,2,5,5-tetramethyl-1-pyrrolidinyloxyl (6) and *cis*-3,4-dicarboxy-2,2,5,5-tetramethyl-1-pyrrolidinyloxy (5), as depicted in Figure 1. Thereafter, endospores (5×10^6/mL) were incubated at 37°C for 18 h either with aminoxyl (5) (5 mM, 0.5% DMSO, final concentration) or aminoxyl (6) (5 mM, 0.5% DMSO, final concentration). After extensive washing, endospores that were treated with aminoxyl (6) but not aminoxyl (5) exhibited an EPR spectrum (Figure 6) that was substantially greater than when endospores were covalently labelled with maleimide-containing aminoxyls (Figure 3). In contrast, endospores exposed to aminoxyl (5) did not exhibit an EPR spectrum (Figure 6). These results suggest that aminoxyl (6) diffused into the exosporium where,

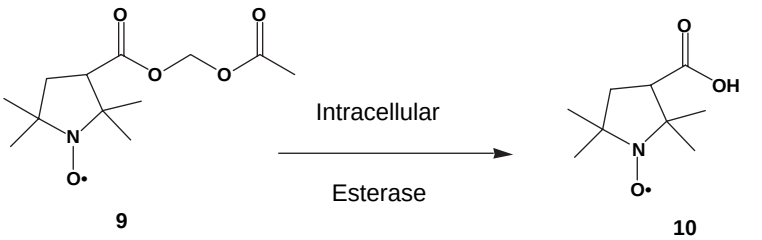

Figure 4. Intracellular esterase hydrolysis of aminoxyl (9) to aminoxyl (10), the latter aminoxyl is entrapped therein due to its anionic character.

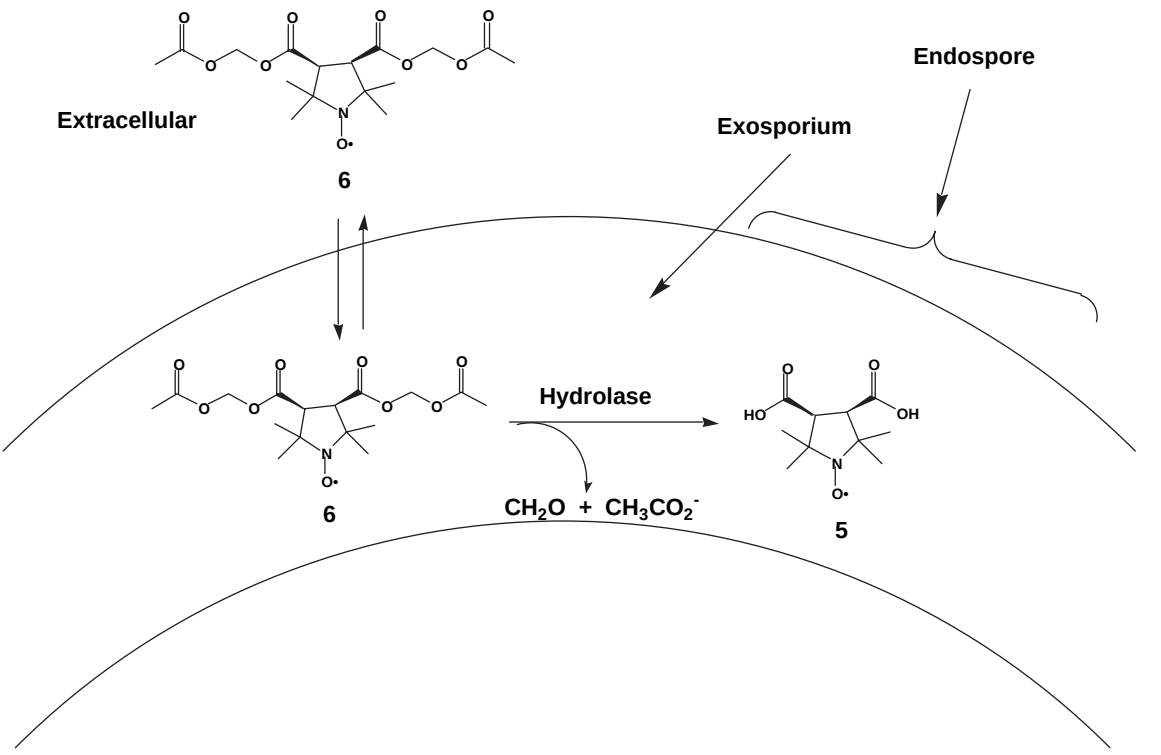

Figure 5. Esterase-assisted loading of aminoxyl (6) into an endospore. Aminoxyl (6) diffuses into an endospore, where it is hydrolysed by a hydrolase, to entrap aminoxyl (5).

after hydrolysis, the dianionic form of aminoxyl (5) was well-retained in the endospore (Figure 5).

One of the hydrolases reported to be in the exosporium is inosine hydrolase [17]. To see if this enzyme might be responsible for the hydrolysis of aminoxyl (6), we treated endospores (3×10^7/mL) with aminoxyl (6) in the presence of inosine (500 μM), a substrate for the hydrolase. After extensive washing the EPR spectral peak height of endospores containing the aminoxyl was significantly smaller than that found for control, in the absence of inosine (Figure 7). Since aminoxyl (6) readily diffuses into and out of the endospore, the concentration of the hydrolysis product, aminoxyl (5), which is entrapped in the exosporium, would be diminished as

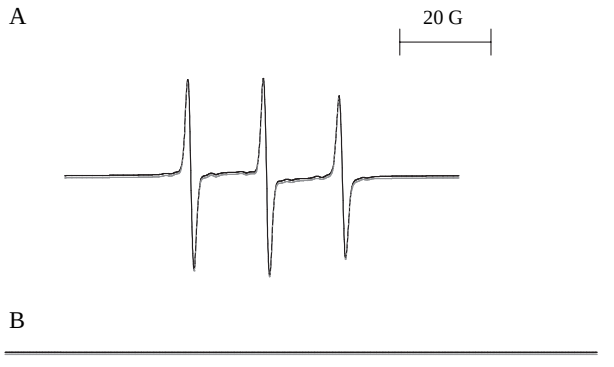

Figure 6. (A) A typical EPR spectrum of aminoxyl (5) entrapped in endospores after exposure to aminoxyl (6). (B) A representative EPR spectrum of incubating endospores with aminoxyl (5). Data shown are the average of 10 scans. Instrumental settings: microwave power, 20 mW; field set, 3330 G; sweep width, 100 G; modulation frequency, 100 kHz; modulation amplitude, 0.5 G; response time, 0.5 s; sweep, 12.5 $Gmin^{-1}$; and receiver gain 4×10^3.

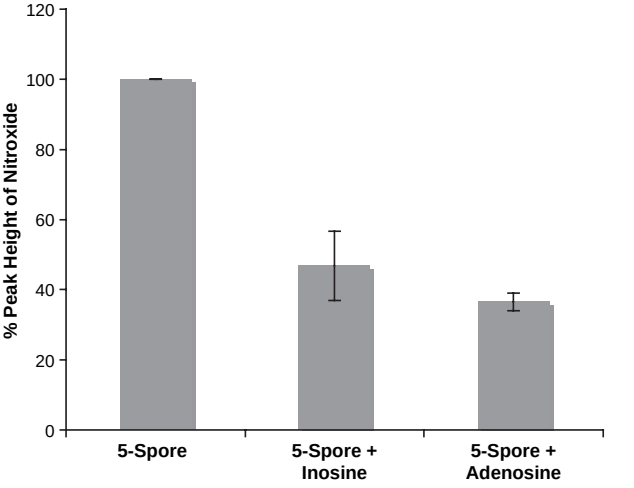

Figure 7. Effect of inosine (500 μM) and adenosine (500 μM) on the peak height of aminoxyl (5) entrapped within endospores. The peak height of the low field EPR spectrum was measured and converted to percentage, where control, in the absence of either inosine or adenosine, was presented as 100%. Each bar on the graph is the average of three independent experiments, expressed as the means and standard deviations. Instrumental settings: microwave power, 20 mW; field set, 3330 G; sweep width, 100 G; modulation frequency, 100 kHz; modulation amplitude, 0.5 G; response time, 0.5 s; sweep, 12.5 $Gmin^{-1}$; and receiver gain 2.5×10^3.

compared to control, in the absence of inosine. This finding suggests that inosine hydrolase preferentially metabolized inosine at the expense of aminoxyl (6). To further verify that inosine hydrolase is responsible for facilitating the formation of aminoxyl (5), an inhibitor of inosine hydrolase, adenosine, was used [21]. In the presence of adenosine (500 μM), the concentration of the entrapped aminoxyl (5) in exosporium was diminished (Figure 7) as compared with the control. Data presented in Figure 7 offer strong evidence that inosine hydrolase was responsible for the hydrolysis of aminoxyl (6), thereby capturing aminoxyl (5) in the exosporium of the endospore.

Loading of RAW 264.7 cell with aminoxyl-labelled/ entrapped endospore

We then infected RAW 264.7 cells (5×10^6/mL) with endospores (5×10^6/mL) that previously had been covalently labelled with either aminoxyl (1) or aminoxyl (6). After incubation for 18 h at 37°C, these macrophages were extensively washed to remove extracellular endospores. The remaining RAW 264.7 cells containing endospores that had previously been covalently labelled with aminoxyl (1) exhibited an EPR spectrum, whose intensity was modest, as shown in Figure 8A. However, in the case of macrophages infected with aminoxyl (5)-entrapped endospores, the EPR signal intensity was substantially higher (Figure 8B) than endospore labelled with aminoxyl (1). As a control RAW 264.7 cells were incubated with either aminoxyl (1) or aminoxyl (5) for 18 h at 37°C. After washing the RAW 264.7 cells, no EPR spectrum was observed (data not shown). These findings point to the fact that endospores containing either aminoxyl (1) or aminoxyl (5) did not inhibit the ability of macrophages to phagocytize aminoxyl-containing endospores. However, more importantly, under these compromising experimental conditions, 18 h at 37°C, aminoxyl-labelled endospores were stable in the harsh environment of the macrophage. The stability of aminoxyl (5) containing endospores in RAW 264.7 cells was further determined by noting that this EPR spectrum remained unchanged for at least 2 h, when the experiment was terminated (data not shown).

We had previously demonstrated that phagocytosis of endospores of *B. anthracis* by RAW 264.7 cells was an actin-dependent process [22]. We were interested in determining whether the labelling of endospores with aminoxyl (5) would alter the mechanism of internalization by macrophages. Thus, RAW 264.7 cells (5×10^6/mL) were incubated with cytochalasin D (10 μg/mL) for 10 min, prior to infection with endospores (5×10^6/mL) containing aminoxyl (5). As shown in Figure 9A, those macrophages that had phagocytized endospores labelled with aminoxyl (5) exhibited an EPR spectrum identical to that observed in Figure 8A. In contrast, when RAW 264.7 cells were pre-incubated with cytochalasin D and then treated with endospores labelled with aminoxyl (5), there was no observable EPR spectrum (Figure 9B). These findings demonstrate that the phagocytosis of aminoxyl-entrapped endospores by RAW 264.7 cells is an actin-dependent process.

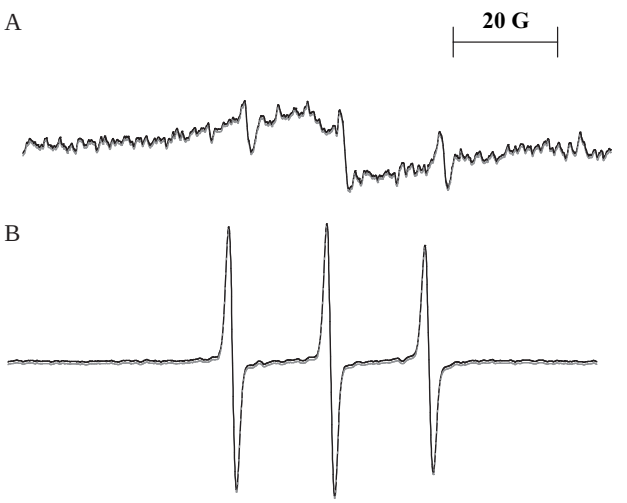

Figure 8. Comparison of the aminoxyl-labelled/entrapped endospores engulfed by RAW264.7 cells (5×10^6/mL). (A) Aminoxyl (1)-labelled endospores (5×10^6/mL) were used. (B) Aminoxyl (5)-entrapped endospores (5×10^6/mL) were used. Data shown are the average of 20 scans. Instrumental settings: microwave power, 20 mW; field set, 3330 G; sweep width, 100 G; modulation frequency, 100 kHz; modulation amplitude, 0.5 G; response time, 0.5 s; sweep, 12.5 Gmin^{-1}; and receiver gain 10×10^4.

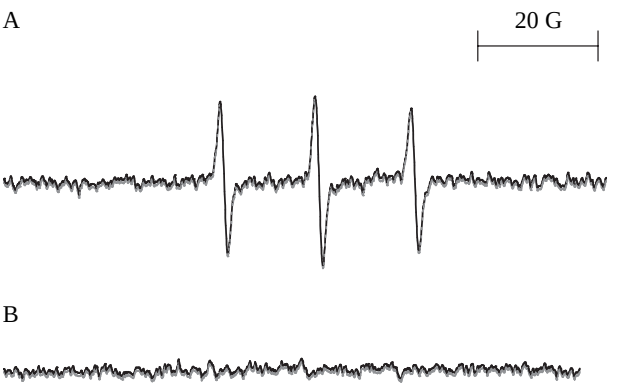

Figure 9. Effect of cytochalasin D on the phagocytosis of aminoxyl (5)-entrapped endospores by the RAW 264.7 cells. (A) Phagocytosis of aminoxyl (5)-entrapped endospores (5×10^6/mL) without the pre-treatment of cytochalasin D. (B) Phagocytosis of aminoxyl (5)-entrapped endospores (5×10^6/mL) with the pre-treatment of cytochalasin D (10 μg/mL). Instrumental settings: microwave power, 20 mW; field set, 3330 G; sweep width, 100 G; modulation frequency, 100 kHz; modulation amplitude, 0.5 G; response time, 0.5 s; sweep, 12.5 Gmin^{-1}; and receiver gain 8×10^4.

Conclusion

In this report we have shown that of the two approaches to incorporate an aminoxyl into endospores, the acetoxymethoxycarbonyl method holds the most promise for *in vivo* detection of endospores by low-frequency EPR spectroscopy. While it is premature to predict the feasibility of *in vivo* EPR imaging of endospore-containing aminoxyl, we [23] have recently imaged by EPR spectroscopy aminoxyl-entrapped within lymphocytes at concentrations similar to what we observe in experiments presented herein. Future *in vivo* kinetic experiments will determine whether it is feasible to track aminoxyl-loaded endospores of *B. anthracis* by low-frequency EPR spectroscopy.

Acknowledgements

This research was supported in part by grants from the National Institutes of Health, EB-2034 and the Mid-Atlantic Regional Center for Biodefense and Emerging Infectious Diseases, NIAID U54 AI-057168.

References

[1] Koch R. Die etiologie der milzbrand krankheit hegrundet auf die entwickelungsgeschichte des *Bacillus anthraci*. Beit Biol Pflanz 1876;2:277–283.
[2] Ross JM. The pathogenesis of anthrax following the administration of spores by the respiratory route. J Pathol Bacteriol 1957;73:485–494.
[3] Shafa F, Moberly BJ, Gerhardt P. Cytological features of anthrax spores phagocytized *in vitro* by rabbit alveolar macrophages. J Infect Dis 1966;116:401–413.
[4] Guidi-Rontani C, Weber-Levy M, Labruyere E, Mock M. Germination of Bacillus anthracis spores within alveolar macrophages. Mol Microbiol 1999;31:9–17.
[5] Dixon TC, Fadl AA, Koehler TM, Swanson JA, Hanna PC. Early *Bacillus anthracis* macrophage interactions: intracellular survival and escape. Cell Microbiol 2000;2:453–463.
[6] Guidi-Rontani C, Levy M, Ohayon H, Mock M. Fate of germinated Bacillus anthracis spores in primary murine macrophages. Mol Microbiol 2001;42:931–938.
[7] Brittingham KC, Ruthel G, Panchal RG, Fuller CL, Ribot WJ, Hoover TA, Young HA, Anderson AO, Bavari S. Dendritic cells endocytose Bacillus anthracis spores: implications for anthrax pathogenesis. J Immunol 2005;174:5545–5552.
[8] Guidi-Rontani C, Pereira Y, Ruffie S, Sirard JC, Weber-Levy M, Mock M. Identification and characterization of a germination operon on the virulence plasmid pXOl of Bacillus anthracis. Mol Microbiol 1999;33:407–414.
[9] Ireland JA, Hanna PC. Macrophage-enhanced germination of Bacillus anthracis endospores requires gerS. Infect Immun 2002;70:5870–5872.
[10] Dalldorf FG, Kaufmann AF, Brachman PS. Woolorters' disease: an experimental model. Arch Pathol 1971;92:418–426.
[11] Halpern HJ, Spencer DP, van Polen J, Bowman MK, Masssoth RJ, Nelson AC, Dowey EM, Teicher BA. An imaging radiofrequency electron spin resonance spectrometer with high resolution and sensitivity for *in vivo* measurements. Rev Sci Instrum 1989;60:1040–1050.
[12] Elas M, Williams BB, Parasca A, Mailer C, Pelizzari CA, Lewis MA, River JN, Karczmar GS, Barth ED, Halpern HJ. Quantitative tumor oxymetric images from 4D electron paramagnetic resonance imaging (EPRI): methodology and comparison with blood oxygen level-dependent (BOLD) MRI. Magn Reson Med 2003;49:682–691.
[13] Baillie L, Hibbs S, Tsai P, Cao G-L, Rosen GM. Role of superoxide in the germination of *Bacillus anthracis* endospores. FEMS Microbiol Lett 2005;245:33–38.
[14] Rozantsev EG. Free nitroxyl radicals. New York: Plenum Press; 1970.
[15] Mathew AE, Dodd JR. Synthesis of substitute, 2,2,5,5-tetramethylpyrrolidin-1-oxyl spin labels—pH sensitivity studies. J Heterocyclic Chem 1985;22:225–228.
[16] Rosen GM, Pou S, Cohen MS, Hassett DJ, Britigan BE, Barber MJ, Cao G-L, Cosby K, Sturgeon BE, Halpern HJ. ^{14}N-Spin trapping of free radicals in the presence of ^{15}N-spin labeled *Neisseria gonorrhoeae*. J Chem Soc Perkin Trans 2 1999;:297–300.
[17] Redmond C, Baillie LWJ, Hibbs S, Moir AJG, Moir A. Identification of proteins in the exosporium of *Bacillus anthracis*. Microbiology 2004;150:355–363.
[18] Keana JFW, Pou S, Rosen GM. Nitroxides as potential contrast enhancing agents for MRI applications: influence of structure on the rate of reduction by rat hepatocytes, whole liver homogenate, subcellular fractions, and ascorbate. Magn Reson Med 1987;5:525–536.
[19] Kocherginsky N, Swartz HM. Nitroxide spin labels. Reaction in biology and chemistry. Boca Raton, FL: CRC Press; 1995.
[20] Kao JPY, Rosen GM. Esterase-assisted accumulation of 3-carboxy-2,2,5,5-tetramethyl-1-pyrrolidinyloxyl into lymphocytes. Org Biomol Chem 2004;2:99–102.
[21] Miller RL, Sabourin CLK, Krenitsky TA. Nucleoside hydrolases from *Trypanosoma cruzi*. J Biol Chem 1984;259:5073–5077.
[22] Raines KW, Kang TJ, Hibbs S, Cao G-L, Weaver J, Tsai P, Baillie L, Cross AS, Rosen GM. Importance of nitric oxide synthase in the control of infection by Bacillus anthracis. Infect Immun 2006;74:2268–2276.
[23] Kao JPY, Barth ED, Burks SR, Smithback P, Mailer C, Ahn K-H, Halpern HJ, Rosen GM. Very-low-frequency electron paramagnetic resonance (EPR) imaging of nitroxide-loaded cells. Magn Reson Med 2007;58:850–854.